Resolving cadherin interactions and binding cooperativity at the single-molecule level

Yunxiang Zhang[a,1], Sanjeevi Sivasankar[b,1,2,3], W. James Nelson[c,d], and Steven Chu[a,b,e,3]

Departments of [a]Physics, [c]Biology, and [d]Molecular and Cellular Physiology, Stanford University, Stanford, CA 94305; [b]Departments of Physics and Molecular and Cell Biology, University of California, Berkeley, CA 94720; and [e]Lawrence Berkeley National Laboratory, Berkeley, CA 94720

Contributed by Steven Chu, November 10, 2008 (sent for review September 13, 2008)

The cadherin family of Ca^{2+}-dependent cell adhesion proteins are critical for the morphogenesis and functional organization of tissues in multicellular organisms, but the molecular interactions between cadherins that are at the core of cell–cell adhesion are a matter of considerable debate. A widely-accepted model is that cadherins adhere in 3 stages. First, the functional unit of cadherin adhesion is a *cis* dimer formed by the binding of the extracellular regions of 2 cadherins on the same cell surface. Second, formation of low-affinity *trans* interactions between cadherin *cis* dimers on opposing cell surfaces initiates cell–cell adhesion. Third, lateral clustering of cadherins cooperatively strengthens intercellular adhesion. Evidence of these cadherin binding states during adhesion is, however, contradictory, and evidence for cooperativity is lacking. We used single-molecule structural (fluorescence resonance energy transfer) and functional (atomic force microscopy) assays to demonstrate directly that cadherin monomers interact via their N-terminal EC1 domain to form *trans* adhesive complexes. We could not detect the formation of cadherin *cis* dimers, but found that increasing the density of cadherin monomers cooperatively increased the probability of *trans* adhesive binding.

atomic force microscope | cell adhesion | *cis* dimer | fluorescence resonance energy transfer | *trans* binding

Cadherins are Ca^{2+}-dependent cell–cell adhesion proteins that play fundamental roles in the functional organization of cells and in maintaining the structural integrity of solid tissues (1, 2). Cadherin adhesion is modified during normal embryonic development, and disruption of adhesion is common in metastatic cancers (2–4). Despite detailed studies of cadherin-mediated adhesion in multicellular organisms, a molecular understanding of the adhesive states of cadherin is less clear (5). Structural studies have shown that cadherin–cadherin contacts are mediated by the extracellular domain comprised of tandem repeats of 5 cadherin (EC) domains. A widely accepted model as summarized in textbooks (6) and recent review articles (1, 7–9) is that the functional unit of cadherin adhesion is a *cis* dimer formed by binding of the extracellular domains of 2 cadherins on the same cell surface. Cell–cell adhesion is initiated by the formation of *trans* adhesive complexes between the EC1 domains of cadherin *cis* dimers on opposing cell surfaces (1, 6–15). Strong cadherin adhesion may also require *trans* binding along additional EC domains (16–19). *Trans*-cadherin binding is a low-affinity interaction, but cell–cell adhesion is believed to be enhanced cooperatively by the lateral clustering of cadherins (20, 21).

Evidence for these *trans*- and *cis*-cadherin binding states, however, is controversial, and evidence for cooperativity in promoting adhesion is lacking. Models of cadherin *cis* dimerization are based on indirect evidence from the packing interactions in cadherin crystal structures (11, 15, 22, 23), electron tomographs of desmosomes (12, 13), electron micrographs of E-cadherin fusion constructs (24), and chemical cross-linking and gel filtration of cadherin extracted from cells (25). Although the cadherin *cis* interaction site was initially localized to the EC1 domains (10, 24), it was later proposed that EC1 and EC2 domains of neighboring cadherin molecules are involved in these interactions (11, 26). However, other studies using protein cross-linking and coimmunoprecipitation demonstrated that *cis* cadherin dimers were formed only in cells grown artificially at low calcium concentrations, and that *cis* and *trans* interactions shared the same adhesive interface (27–29). Although some electron tomography experiments have shown *trans* interactions involving both cadherin monomers and *cis* dimers (13), other cryoelectron tomographs suggest that *cis* dimerization is mandatory for *trans* adhesion (12). Furthermore, *trans* binding between cadherin monomers was measured by single-molecule force measurements (30), although these experiments could not directly confirm the oligomerization states or extracellular domains of cadherin involved in these interactions.

Unlike the contradictory data on *cis* dimers, there is a better, albeit incomplete, understanding of how *trans* interactions occur between cadherins on opposing cell surfaces. Electron microscopy (12, 13, 24, 31), X-ray crystallography (10, 11, 15, 22), NMR (26, 32), mutational experiments (22), and domain swapping experiments (33) have implicated the EC1 domain in cadherin *trans* interactions. However, direct force measurements (16–18) supported by cell attachment and bead binding assays (19) showed 3 distinct adhesive alignments interpreted as the overlap of opposing EC1-5, EC1-3, and EC1 domains. Furthermore, mAbs against the EC4/EC5 domains block cell–cell adhesion (34, 35). These data raise questions about the EC domains that participate in *trans* cadherin binding.

Trans binding interactions have a remarkably low affinity (K_D $\approx$720 μM in 1 mM Ca^{2+} and K_D $\approx$10 mM in 0 mM Ca^{2+}) (26) considering their role in cell–cell adhesion. It is generally thought that weak *trans* binding is enhanced cooperatively by clustering of cadherins on the cell surface (20). However, such cooperativity has not been measured directly.

These conflicting data on the molecular characteristics of cadherin binding states can be resolved by identifying binding interfaces and measuring adhesion between cadherin monomers and dimers. Such studies are tricky in live cells because it is difficult to monitor the structure and function of asynchronously adhesive subpopulations of cadherin molecules. Therefore, we sought to approach these problems by establishing a series of single-molecule in vitro assays to directly detect cadherin monomers and *cis* dimers, identify the EC domains involved in the *trans* adhesive state, and measure cooperativity in *trans* cadherin adhesion.

Author contributions: Y.Z., S.S., W.J.N., and S.C. designed research; Y.Z. and S.S. performed research; Y.Z., S.S., W.J.N., and S.C. analyzed data; and S.S. wrote the paper.

The authors declare no conflict of interest.

[1]Y.Z. and S.S. contributed equally to this work.

[2]Present address: Department of Physics and Astronomy, Iowa State University, Ames, IA 50011.

[3]To whom correspondence may be addressed. E-mail: sivasank@iastate.edu or schu@lbl.gov.

This article contains supporting information online at www.pnas.org/cgi/content/full/0811350106/DCSupplemental.

Results and Discussion

To examine the orientation (*cis* vs. *trans*) and number of EC domains involved in cadherin–cadherin interactions, we measured FRET between functional E-cadherin extracellular domains. The aspargine residue at position 20 on the EC1 domain of E-cadherin was mutated to a cysteine residue (N20C), and the C-terminal at the EC5 domain was fused to a biotin or hexa-his affinity tag for protein purification and functional surface immobilization. Cy3 and Alexa Fluor 647 FRET dye labels were attached to the engineered cysteine residue in the EC1 domain. The biological activity of all of the cadherin constructs used in these experiments was verified in standard assays by monitoring Ca^{2+}-dependent aggregation of cadherin functionalized beads (19, 33) (described in *Materials and Methods* and Fig. S1).

The oligomeric state of fluorophore-labeled cadherin was confirmed by immobilizing molecules on a surface, exciting the fluorophores, and monitoring discrete photo-bleaching steps (Fig. S2). Because the dye to protein labeling efficiency was 60–90%, cadherin monomers should photo-bleach in a single step. More than 85% of cadherin molecules exhibited single photo-bleaching events (Fig. S2). Multiangle laser light scattering confirmed the oligomeric states of the cadherin monomers and dimers (data not shown).

Because cadherin–cadherin binding has low affinity (26), we used chemical cross-linking in solution to stabilize transient interactions between donor- and acceptor-labeled cadherin monomers (Fig. 1*A*). The cross-linking yield doubled from 20% to 40% when the Ca^{2+} concentration was increased from 0 to 0.1 mM and remained constant when the Ca^{2+} concentration was increased from 0.1 to 1 mM (Fig. S3). Cross-linked cadherins were immobilized on a surface and observed in total internal reflection geometry with single-molecule sensitivity (Fig. 1*B*). FRET data were analyzed only from molecules containing colocalized donor and acceptor fluorophores were determined by using sequential 2-color excitation (described in *Materials and Methods*). Cadherin cross-linked in 0 mM Ca^{2+} did not exhibit a high FRET signal (Fig. 1*C*). However, a majority of cadherin cross-linked in 0.1, 0.5, or 1 mM Ca^{2+} exhibited a high FRET value of 0.8 (Fig. 1 *D–F*). This FRET value corresponds to a distance of ≈4 nm between the donor and acceptor fluorophores on the cadherin EC1 domains. Because cross-linking was performed in solution before surface immobilization, this high FRET signal could have arisen through proteins interacting via their EC1 domains in either *cis* or *trans* geometry (Fig. 1*A*).

To distinguish between *cis* and *trans* dimers, the COOH terminus of the cadherin extracellular domain was fused to the Fc domain of human IgG1 (Fig. 2*A*). The 20-aa hinge region linking the cadherin monomers to the dimerized Fc served as a flexible tether (36, 37) that allowed the cadherin pair to form a close *cis* orientation through the dimerized Fc domain (19, 38). The oligomeric state of fluorophore-labeled cadherin–Fc dimers was confirmed by immobilizing molecules labeled with only donor fluorophores on a surface, exciting the fluorophores, and monitoring discrete photo-bleaching events. Approximately 60% of the cadherin–Fc dimers in 1 mM Ca^{2+} showed colocalized fluorescent spots, whereas the remaining molecules showed >2 discrete photo-bleaching steps, either caused by *trans* binding or neighboring molecules becoming immobilized at optically unresolvable distances (Fig. S2). To monitor the distance between EC1 domains of the cadherin–Fc dimers, they were dual-labeled with donor and acceptor fluorophores and immobilized on a surface, and their FRET signal was monitored at 2 different calcium concentrations (Fig. 2*A*). Very few high FRET signals were observed at 0.1 and 1 mM Ca^{2+} (results of 1 mM Ca^{2+} measurement are shown in Fig. 2*B*).

To confirm that the cadherins in the Fc dimer construct were not sterically hindered from interacting with each other, the cadherins were chemically cross-linked to trap transient molecular interactions (Fig. 2*C*). Only a small increase in the frequency of FRET events is expected in sterically unhindered, noninteracting cadherin pairs because most transient collisions would not show a FRET signal. A broad distribution of FRET values was observed, with 7% of the samples showing high FRET (Fig. 2*D*). This finding confirms that the cadherin pairs in the Fc dimer have sufficient collisional freedom and are not sterically hindered from forming *cis* dimers.

The cadherin–Fc dimer experiments demonstrate that cadherins placed in close proximity to each other in a *cis* orientation do not interact via their outermost EC1 domains or do not exist at all. Therefore, we conclude that the high FRET signal observed with cross-linked cadherin monomers (see Fig. 1 *D–F*) arose through proteins interacting via a *trans* orientation, rather than a *cis* orientation of their EC1 domains. These single-molecule FRET experiments provide direct evidence that cadherin *cis* dimers are not necessary for *trans* cadherin adhesion. In contrast to these single-molecule experiments, electron micros-

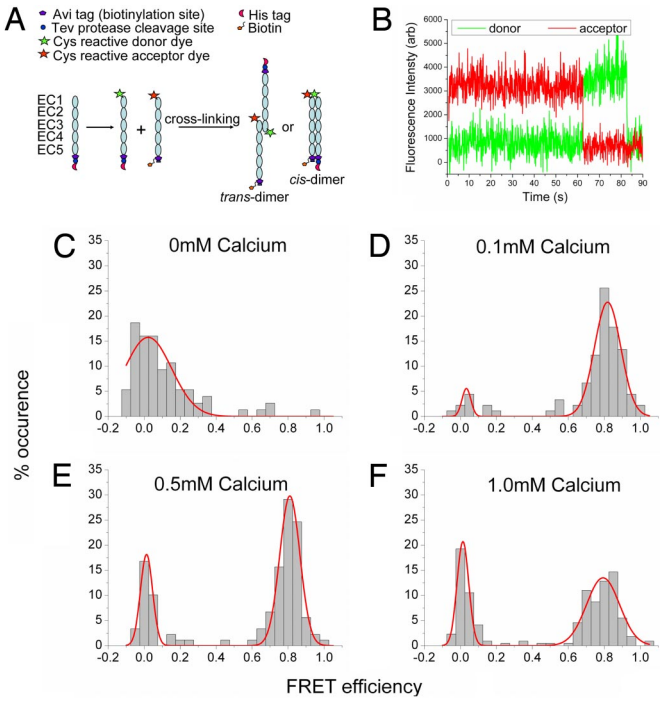

Fig. 1. Cadherin monomers interact via their outermost (EC1) domain. (*A*) Steps involved in cross-linking EC1-labeled cadherin monomers. An aspargine residue at position 20 on the EC1 domain of E-cadherin was mutated to a cysteine residue (N20C). The cadherin monomers engineered with a His affinity tag or a biotin tag were labeled with a donor Cy3 fluorophore or acceptor Alexa Fluor 647 fluorophore, respectively. Donor- and acceptor-labeled cadherins were cross-linked in solution by using an amine reactive BS3 cross-linker. Cross-linking reactions were carried out in buffers containing Ca^{2+} concentrations of 0, 0.1, 0.5, and 1 mM; cross-linked dimer yields at these Ca^{2+} concentrations were 20%, 40%, 32%, and 49% respectively. Cross-linked cadherin dimers were immobilized on a surface. (*B*) Typical fluorescence time trace from a dual-labeled cross-linked cadherin dimer showing a 0.8 FRET efficiency. This FRET efficiency corresponds to a distance of 4 nm between donor and acceptor fluorophores on the EC1 domain. When the donor fluorophore is excited at time = 0 s, it nonradiatively transfers energy to the acceptor fluorophore (red trace). The donor fluorescence (green trace) is recovered when the acceptor photobleaches (at ≈62 s). The FRET efficiency is calculated from the ratio of the acceptor and donor fluorescence intensities. (*C–F*) Histogram of FRET efficiencies for cadherin dimers cross-linked at different Ca^{2+} concentrations. At 0.1, 0.5, and 1.0 mM Ca^{2+} we observe 84%, 70%, and 60%, respectively, of the colocalized fluorescence spots have high FRET values.

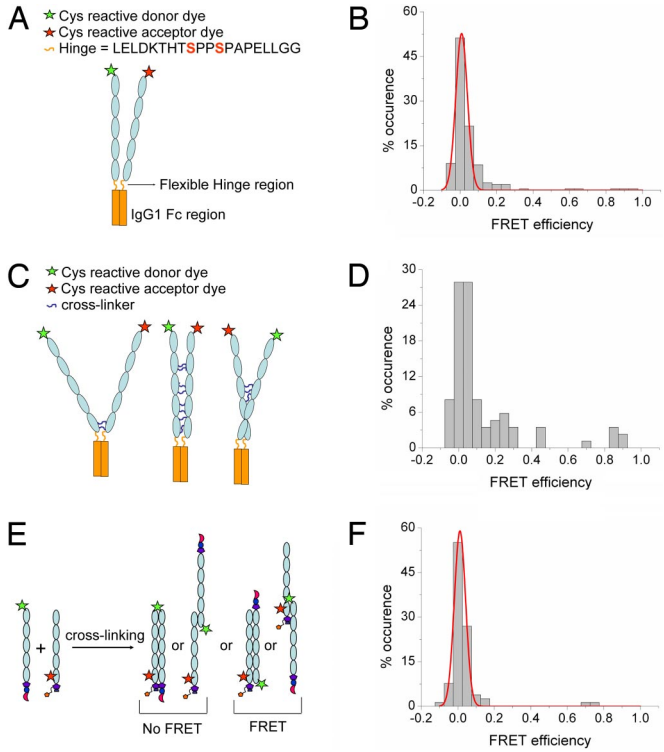

Fig. 2. Cadherins do not form *cis* dimers. *Trans* dimerization is mediated by the outermost EC1 domain. (*A*) Schematic of cadherin–Fc dimer construct. The cadherin–Fc dimer construct was engineered by fusing the COOH terminus of the cadherin extracellular region to the Fc domain of human IgG1. Engineered cysteines on the EC1 domains of the cadherins were dual-labeled with donor and acceptor fluorophores. The cysteine residues in the core hinge region were mutated to serines to prevent nonspecific labeling of the Fc dimer. The cadherin–Fc dimers were immobilized on a surface, and their FRET signal was monitored at 0.1 and 1 mM Ca^{2+}. (*B*) Histogram of FRET efficiencies for cadherin–Fc dimers measured in 1 mM Ca^{2+} for those samples that had both donor and acceptor labels. These dimers show very few events with a FRET efficiency >0.5. (*C*) Schematic of the cross-linked cadherin–Fc dimer construct. The cadherin–Fc dimer was cross-linked in solution with an amine reactive BS3 cross-linker to trap transient collisions between cadherin molecules and to confirm that the cadherins were not sterically hindered from interacting with each other. (*D*) Histogram of FRET efficiencies for the cross-linked cadherin–Fc dimers measured in 1 mM Ca^{2+} showing an increase in high FRET events. (*E*) The EC1 domain of cadherin engineered with a His affinity tag was labeled with a donor fluorophore, whereas the EC5 domain of the cadherin monomer engineered with a biotin was labeled with an acceptor fluorophore. The donor- and acceptor-labeled cadherins were cross-linked in solution. A high FRET signal is expected only if the EC1 and EC5 domains in the cross-linked dimer overlap as shown. (*F*) Histogram of FRET efficiencies for cadherin dimers cross-linked in 1 mM Ca^{2+}. These dimers show very few events with a FRET efficiency >0.5. This result and the results shown in Fig. 1 *D–F* confirms that the cadherin *trans* adhesive complex is formed by the interaction of EC1 domains.

copy of pentameric fusion constructs of E-cadherins revealed ring-like structures between 0.5 and 1.0 mM Ca^{2+} that were interpreted as the association of cadherin molecules in a *cis* orientation through their N-terminal EC1 domains. Adhesive *trans* interactions between pentamers were observed only between ring structures at Ca^{2+} concentrations >1.0 mM, suggesting that the lateral *cis* dimer were the functionally unit of adhesion and *trans* interactions require a high Ca^{2+} concentration (14, 15).

We next examined whether cadherin EC domains other than EC1 are involved in *trans* adhesion. We tested whether there was full interdigitation of cadherin extracellular domains in the *trans* dimers (16, 17) (Fig. 2*E*) by assaying FRET between overlapping EC1 and EC5 domains. The EC5 domain of the cadherin monomer was engineered with a cysteine residue and labeled with an acceptor Alexa Fluor 647 dye. These acceptor-labeled cadherin monomers were cross-linked with cadherin monomers labeled with EC1 domain donor Cy3 fluorophores (Fig. 2*E*). These cadherin dimers cross-linked in 1 mM Ca^{2+} had very few high FRET events (Fig. 2F). This result shows that the EC1 and EC5 domains of opposing cadherins do not overlap in the *trans* adhesive complex and confirms the principle role of EC1 domains in the *trans* binding state (10–13, 15, 24, 26). The experiments, however, do not address whether there is an overlap between other domains as suggested by surface force measurements (16, 17).

To compare the adhesive interactions between cadherin monomers and cadherin–Fc dimers, we measured cadherin–cadherin binding at the single-molecule level by using atomic force microscopy (AFM) (Fig. 3 *A* and *B*). Cadherin–Fc dimers (Fig. 3*A*) or cadherin monomers (Fig. 3*B*) were immobilized on the AFM tip and substrate at identical surface densities of 34 ± 16 dimers per μm^2 and 65 ± 18 monomers per μm^2, and the binding of single cadherin molecules was measured (Fig. 3*C*). The low cadherin surface densities precluded the formation of multivalent interactions between cadherins on the tip and surface because the average distance separating neighboring cadherins (171 and 124 nm for the dimers and monomers, respectively) is significantly larger than the length of the PEG–protein–cadherin assembly anchored to the surface (40 nm for the cadherin-Fc dimer and 35 nm for the cadherin monomer). The frequency of binding events decreased significantly when Ca^{2+} was chelated by the addition of EGTA (Fig. 3 *D* and *E*). Histograms of cadherin monomer (Fig. 3*E*) and cadherin–Fc dimer (Fig. 3*D*) binding showed that both adhesive complexes had similar bond strengths of 64 pN ± 27 pN and 53 pN ± 27pN, respectively; these binding forces are similar to AFM measurements of vascular endothelial–cadherin–Fc dimers (39). Because an adhesive complex formed by cadherin *cis* dimers is nominally expected to be twice as strong as that formed by cadherin monomers, this result provides functional evidence that Ca^{2+}-dependent *trans* adhesive complexes are formed by binding of cadherin monomers and not by cadherin *cis* dimers. Because only 1 cadherin from each Fc–dimer pair participates in the formation of a *trans* dimer, it is possible that the second cadherin may be sterically inhibited from interacting in a *trans* conformation.

Although their bond strengths are similar, the cadherin–Fc dimer had a 3.4-fold higher probability of binding than a cadherin monomer (Fig. 3 *D* and *E*). Whereas 6.4% of cadherin–Fc dimer force measurements yielded binding events, only 1.9% of cadherin monomer force measurements resulted in binding. This finding is unexpected because pairs of cadherin monomers that interact independently of each other are expected to have a 2-fold higher binding probability than unpaired monomers at identical protein surface densities. The 3.4-fold higher binding probability indicates that the paired cadherin monomers in the Fc dimer cooperatively enhance the probability of binding.

Finally, we tested whether this enhanced binding probability depended on the interaction time between the cadherins on the AFM tip and cadherins on the surface. However, we found that at tip–surface contact times of 1,100, 340, and 115 ms the enhancement of cadherin–Fc dimer binding probabilities were similar (3.5, 3.1, and 3.6 times higher, respectively, than the probability of monomer interactions), demonstrating that the enhancement of binding probability was independent of interaction time.

A widely-accepted model that has emerged from previous studies of cadherin interactions is that cadherin *cis* dimers form initially weak *trans* adhesion complexes (5, 10–13, 15, 22–26), which are subsequently strengthened cooperatively by cadherin clustering (20). Here, we tested directly the functional organi-

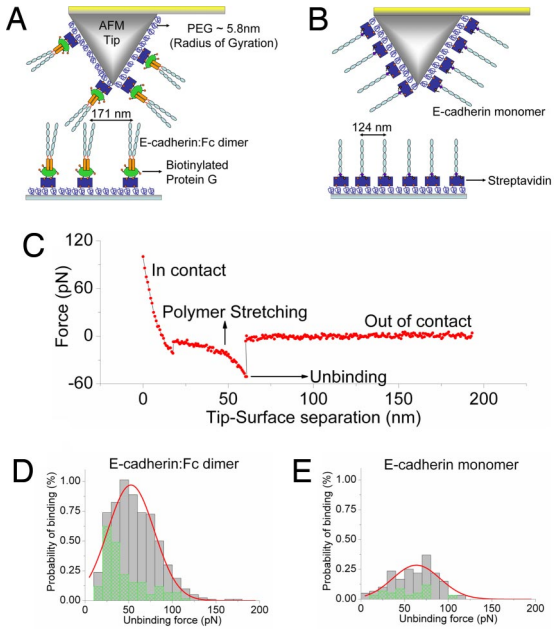

Fig. 3. Close proximity of cadherin molecules in a *cis* orientation cooperatively increases the probability of *trans* cadherin binding. (*A*) Schematic of AFM tip and substrate functionalized with cadherin–Fc dimers for single-molecule force measurements. The tip and surface were functionalized with PEG linkers, some of which were decorated with streptavidin molecules. Cadherin–Fc dimers were immobilized on biotinylated protein G attached to the streptavidin molecules on the tip and surface. The flexible PEG linkers enable unhindered interactions between opposing cadherins during tip–substrate encounters. Cadherin–Fc dimers were immobilized on the AFM tip and substrate at a surface density of 34 ± 16 dimers per μm^2. (*B*) Schematic of AFM tip and substrate functionalized with biotinylated cadherin monomers for single-molecule force measurements. The biotinylated cadherin monomers were immobilized on an AFM tip and substrate via streptavidin-PEG tethers at a surface densities of 65 ± 18 monomers per μm^2; thus, the protein surface density for the cadherin monomers and cadherin–Fc dimer constructs are similar. (*C*) A typical force curve showing the unbinding of a single cadherin molecule. The tip and the substrate decorated with cadherins were bought into contact for either 1,100, 340, or 115 ms so that cadherins on the tip and substrate formed an adhesive complex. When the tip was withdrawn from the substrate a force was exerted, and above a critical force the adhesive complex ruptured. Forces between the cadherin–Fc dimers were measured 7,995 times in 2.5 mM Ca^{2+}, yielding 509 binding events, and 5,931 times in 2 mM EGTA, yielding 123 binding events. Forces between the cadherin monomers were measured 5,949 times in 2.5 mM Ca^{2+}, yielding 113 binding events, and 5,846 times in 2 mM EGTA, yielding 28 binding events. (*D*) Histogram of cadherin–Fc dimer binding events measured in 2.5 mM Ca^{2+} (solid gray bars) and 2 mM EGTA (hatched green bars). The binding events measured in 2.5 mM Ca^{2+} were fitted to a Gaussian distribution with a peak force of 53 ± 27 pN. The binding probability of cadherin–Fc dimers at contact times of 1,100, 340, or 115 ms was 8.6%, 6.6%, and 3.7%, respectively. The histogram includes the forces measured at all 3 tip-surface contact times. (*E*) Histogram of cadherin monomer binding events measured in 2.5 mM Ca^{2+} (solid gray bars) and 2 mM EGTA (hatched green bars). The histogram includes the forces measured at all 3 tip-surface contact times (see above). The binding events measured in 2.5 mM Ca^{2+} were fitted to a Gaussian distribution with a peak force of 64 ± 27 pN. Although the bond strengths of the monomer and cadherin–Fc dimer adhesive complexes are similar, the cadherin–Fc dimer has a higher probability of binding than a cadherin monomer. The total probability of cadherin monomer binding at contact times of 1,100, 340, or 115 ms was 2.5%, 2.2%, and 1.1% respectively. Thus, the cadherin–Fc dimer binding probability was 3.5, 3.1, and 3.6 times higher than the probability of monomer interactions at these tip-surface contact times.

zation of cadherin adhesive states by using single-molecule FRET and AFM force measurements with engineered E-cadherin monomers and dimers. Our results show that cadherin monomers interact via their EC1 domains to form *trans* adhesive complexes. This *trans* cadherin adhesion does not require the prior formation of cadherin *cis* dimers; indeed the probability of *cis* dimer formation is extremely low, even when 2 cadherins are very closely associated at their C terminals. However, we found that close proximity (clustering) of cadherin molecules in a *cis* orientation cooperatively increased the probability of *trans* cadherin binding. Together, our results provide direct, quantitative evidence that cadherin binding involves 2 stages: a weak *trans* binding through EC1 domains and an increased strengthening of adhesion by lateral clustering of cadherins.

Materials and Methods

Cloning and Expression of E-cadherin Constructs. E-cadherin monomer constructs were engineered by a standard 2-step cloning procedure. The full extracellular region of E-cadherin including the signaling sequence was first cloned into a PAC4 vector (Avidity) with a C-terminal Avi tag. The E-cadherin sequence with the Avi tag was then cloned back into the original expression vector by using primers containing a Tev sequence and His tag, which resulted in an ORF of the complete cadherin/Avi/Tev/His (E-cadherin/ATH) sequence.

Synthesis of the E-cadherin/Fc construct with the extracellular domain of E-cadherin (complete with upstream signaling sequence) fused to the hinge and constant region of human IgG1 has been described (38). To provide a more flexible hinge region and avoid nonspecific dye labeling, the cysteine residues in the core hinge were mutated to serines. A surface-accessible cysteine (N20C or Q523C) was introduced on either the EC1 or EC5 domain of both E-cadherin/Fc and E-cadherin/ATH by point mutation by using a QuikChange kit (Stratagene).

Cadherin sequences incorporated into the pcDNA3.1(+) vectors were transfected into HEK 293 cells that were selected by using 400 μg/ml of Genecitin (G418; Invitrogen). Cells were grown to confluency in high-glucose DMEM containing 10% FBS and 200 μg/mL G418 and then exchanged into serum-free DMEM. Conditioned media were collected 4 days after media exchange. Cell debris was cleaned out by centrifugation and filtration through a 0.2-μm membrane.

Purification of E-cadherin Constructs. Fc-cadherin dimers were purified by passing the filtered conditioned media over a column packed with protein A-coated CL-4B Sepharose resin (GE Healthcare). Protein bound to the resin was eluted with 0.2 M Glycine buffer at pH 2.6 and neutralized immediately by 1 M Tris buffer at pH 8.0.

Media containing His-tagged E-cadherin monomers were incubated with nickel-NTA resin (Invitrogen) for 2 h, washed with 50 mM Imidizole to remove nonspecifically-bound protein, and eluted with 250 mM Imidizole. The Fc dimer and monomer constructs were further purified by running through a Superdex200 10/300 GL size exclusion column (GE Healthcare) equilibrated with 25 mM Hepes buffer at pH 7.4 containing 100 mM NaCl, 10 mM KCl, and 1 mM $CaCl_2$.

Bead Aggregation Assays. Biological activity of the cadherin constructs were demonstrated by monitoring the aggregation and disaggregation of cadherin-functionalized beads in the presence or absence of Ca^{2+}, respectively. E-cadherin His-tag monomers were incubated with Cobalt-based Dynabeads Talon (Invitrogen) at 4 °C for 30 min and washed 3 times in a 50 mM Tris buffer at pH 7.4 containing 100 mM NaCl, 10 mM KCl, and 0.2% (wt/vol) BSA (buffer TB). Before incubation, buffer TB was passed over a Chelex 100 resin (Bio-Rad) to chelate out Ca^{2+}. The cadherin-coated beads were then incubated with either the Ca^{2+}-free TB buffer or TB buffer containing 1.8 mM Ca^{2+} for 1 h with constant agitation. Whereas the E-cadherin His-tag monomer-coated beads in 1.8 mM Ca^{2+} showed significant bead aggregation, the beads incubated in the Ca^{2+}-free buffer showed little aggregation (Fig. S1 *a* and *b*).

The biological activity of cadherin–Fc dimers was similarly assayed by their ability/inability to aggregate protein A-decorated Dynabeads (Invitrogen) in the presence of Ca^{2+}/EGTA. The cadherin–Fc dimers were bound to the beads at 4 °C for 30 min and washed 3 times in a 50 mM Tris buffer at pH 7.4 containing 100 mM NaCl, 10 mM KCl, and 0.2% (wt/vol) BSA (buffer TB). The beads were then incubated with buffer TB containing either 1.8 mM Ca^{2+} or 2 mM EGTA (to chelate out calcium) for 1 h with constant agitation. Whereas the cadherin–Fc-coated beads in 1.8 mM Ca^{2+} showed significant bead aggregation, the beads incubated in 2 mM EGTA showed little aggregation (Fig. S1 *c* and *d*).

Determining Molecular Weight of E-cadherin Constructs Using Size Exclusion Chromatography-Multiangle Laser Light Scattering (SEC-MALLS). A DAWN EOS MALLS system (Wyatt Technology) with a K5 flow cell and a 690-nm wavelength laser was used in the light-scattering experiments. Refractive index measurements were performed with an OPTILAB DSP instrument (Wyatt Technology) with a P10 cell. A value of 0.182 mL/g was assumed for the dn/dc (refractive index/protein concentration) ratio of the protein. Samples at ≈2 mg/mL were passed over a Shodex-804 size exclusion column at 0.5 mL/min. Monomeric BSA was used to normalize the detector responses. Astra software (Wyatt Technology) was used to analyze the light-scattering data. The SEC-MALLS experiments confirmed that the molecular mass of the E-cadherin monomer and E-cadherin Fc dimer were 78 ± 4 and 218 ± 13 kDa, respectively (molecular mass of Fc dimer is 51 kDa).

Fluorescent Labeling of E-cadherin Constructs. All fluorescent dye labeling was done in a 25 mM Hepes buffer at pH 7.4 with 100 mM NaCl, 10 mM KCl, and 1 mM $CaCl_2$. A 10-fold molar excess of pH-neutral tris(2-carboxyethyl)phosphine (TCEP) (Pierce Biotechnology) was added to the protein sample to reduce the surface-accessible cysteine residues introduced by point mutation. After 10-min incubation with TCEP, a 10- to 20-fold molar excess of Cy3 maleimide (GE Healthcare) or Alexa647 maleimide (Invitrogen) was added into the labeling mix, and the reaction was incubated for 2 h in the dark at ambient temperature with gentle and constant agitation. Cadherin–Fc dimer molecules were dual-labeled with Cy3 maleimide and Alexa647 maleimide dyes dissolved in DMSO in a 1:1 molar ratio. Dye-labeled cadherin was separated from free dye by using a Superdex 200 10/300 GL column at 4 °C. Labeling efficiency was quantified by measuring the protein concentration (absorption at 280 nm) and dye concentration (absorption maxima of 550 nm for Cy3 and 651 nm for Alexa647 dyes).

Biotinylation of E-cadherin Monomers. A 40-μM solution of cadherin monomers suspended in a pH 7.4 buffer containing 25 mM Hepes, 5 mM NaCl, and 1 mM CaCl2 was biotinylated with BirA enzyme (BirA500 kit; Avidity). After 1-h incubation at 30 °C, free biotins were separated by using a Superdex200 10/300 GL column.

Cross-Linking of Cadherin Monomers. His-tagged cadherin monomers labeled with Cy3 dye and Alexa647-labeled biotinylated cadherin monomers were cross-linked in solution to capture transient interactions between the proteins. Before cross-linking, the His tag was cleaved off the biotinylated cadherin by using AcTev protease (Invitrogen). The dye-labeled cadherins were mixed in equimolar concentrations, incubated on ice for 30 min, concentrated to 80 μM, and cross-linked by using 1 mM amine reactive BS3 cross-linker (Pierce Biotechnology) for 30 min. The cross-linking reaction was quenched with 1 M pH 8.0 Tris buffer. Cross-linked dimers and non-cross-linked monomers were separated by using a Superdex 200 10/300 GL column. The cross-linked dimer yield was measured by absorption at 280 nm as the protein eluted of the sizing column. Cross-linking reactions were carried out in buffers containing 0, 0.1 0.5, and 1 mM calcium. The cross-linked dimer yields at these calcium concentrations were 20%, 40%, 32%, and 49% respectively (Fig. S3).

Total Internal Reflection Fluorescence Microscopy. Quartz slides and glass coverslips were cleaned by heating them at 60 °C for 60 min in a 25% H_2O_2/75% H_2SO_4 solution. The surfaces were rinsed in deionized water and then sonicated for 15 min first in a 1 M potassium hydroxide solution and then in deionized water. Flow cells were constructed by bonding the quartz slides and coverslips together with double-sided sticky tape.

The surface of the flow cell was functionalized with biotin groups by nonspecifically incubating it with biotinylated BSA (0.2 mg/mL for 15 min). The biotins on the BSA were decorated with streptavidin molecules (Pierce Biotechnology) that was used to immobilize cross-linked cadherin dimers. To immobilize Fc–cadherin dimers, the streptavidins were decorated with biotinylated protein G (Pierce Biotechnology), and the Fc region of the cadherin dimer was specifically bound to the protein G.

Fluorescently-labeled cadherin molecules were observed by using a home-built prism-type total internal reflection fluorescence microscope. The donor- and acceptor-labeled molecules were excited by using a diode-pumped 532-nm laser or a 633-nm diode laser. Fluorescence emission was collected by using a 60×, 1.2 NA water-immersion objective and imaged onto a cooled, back-thinned Electron Multiplying CCD camera. Fluorescence lifetimes of Cy3 and Alexa647 dyes were increased by using protocatechuic acid (PCA)/protocatechuate-3,4-dioxygenase (PCD) (Sigma–Aldrich) oxygen scavenger system (40) plus a triplet state quencher/blinking suppressant Trolox (41). The molecules were imaged in a pH 7.4 buffer containing 25 mM Hepes, 100 mM NaCl, 10 mM KCl, 2.5 mM PCA, 50 nM PCD, and 2 mM trolox.

Determining Protein Oligomeric State from Photobleaching Counts. The oligomeric state of the labeled protein was determined by immobilizing the molecules on a surface, exciting the fluorophores, and monitoring their photobleaching (Fig. S2 *a* and *d*). Because the dye-to-protein labeling ratio was typically between 60% and 90%, monomers photobleach in a single discrete step (Fig. S2*b*), whereas dimers show a 2-step photobleaching (Fig. S2*e*). Fluorescence time traces were obtained by using the total internal reflection fluorescence microscope, the number of photobleaching steps was recorded for each individual molecule, and histograms were built to visualize the photobleaching step distribution. A correction was made to take the dye-to-protein labeling efficiency into account.

More than 85% of the cadherin molecules were observed to photobleach in a single step (Fig. 3*C*). Approximately 60% of the cadherin–Fc dimers in 1 mM Ca^{2+} showed colocalized fluorescent spots, whereas the remaining molecules showed >2 discrete photobleaching steps either caused by *trans* binding or because neighboring molecules were immobilized at optically unresolvable distances (Fig. S2*f*).

FRET Analysis. FRET data were acquired only from molecules containing colocalized donor and acceptor fluorophores. The fluorescent molecules were identified by locating fluorescent intensity peaks. Molecules in donor and acceptor channels were registered to subpixel accuracy by 2D polynomial mapping. Fluorescence time traces were calculated by integrating pixels within a radius of ≈1 wavelength from the peak pixel. Colocalized fluorophores were identified by initially locating the acceptor fluorophores by using a 0.5-s excitation with a red laser, then exciting the donor fluorophores and observing FRET by using a ≈30- to 100-s irradiation with the green laser and finally confirming the location of the acceptor by using a 3-s illumination with the red laser. Each colocalized molecule was assigned a FRET value by fitting the histogram of the FRET time trace or by averaging the FRET values of all time points before photobleaching. Final FRET histograms were built based on assigned FRET values of all colocalized molecules.

Sample Preparation for Force Measurements. The cadherin monomers and cadherin–Fc dimer molecules were immobilized on glass coverslips and the Si tip of an AFM cantilever (Olympus). The AFM cantilevers and glass coverslips were cleaned by heating them at 60 °C for 30 min in a 25% H_2O_2/75% H_2SO_4 solution. The cantilevers and coverslips were first rinsed in deionized water and then immersed for 10 min in a 1 M potassium hydroxide solution, then in deionized water and finally in acetone. The AFM cantilevers and coverslips were functionalized with amine groups by using a 2% (vol/vol) solution of 3-aminopropyltriethoxysilane (Sigma) dissolved in acetone. The silanized cantilevers and coverslips were functionalized with PEG spacers (PEG 5000; Laysan Bio) containing an amine-reactive *N*-hydroxysuccinimide ester at 1 end. One percent of the PEG spacers presented biotin molecules on their other end.

These biotins were incubated with 0.1 mg/ml streptavidin for 30 min. The biotinylated cadherin monomers were bound to the streptavidin molecules on the AFM tip and surface. The cadherin–Fc dimer construct was immobilized on biotinylated protein G that was attached to the streptavidin molecules on the tip and surface.

The cadherin monomer surface density was determined by binding a mixture of fluorescently-labeled and unlabeled cadherin monomers in a 1:25 stoichiometry on the functionalized glass coverslip and counting the number of fluorescent spots by using a home-built confocal microscope. The cadherin–Fc dimer surface density was determined by binding a 1:20 stoichiometric mixture of fluorescently-labeled and unlabeled cadherin dimers on the glass coverslip and counting the number of fluorescent spots.

Single-Molecule Force Measurements. The spring constants of the AFM cantilevers were measured with the thermal fluctuation method (42). Forces between single cadherin molecules were measured with an Agilent 5500 AFM in a pH7.5 buffer (10 mM Tris, 100 mM NaCl, 10 mM KCl,) in either 2.5 mM $CaCl_2$ or 2 mM EGTA. The tip and the substrate decorated with cadherins were bought into contact for either 1,100, 340, or 115 ms so that cadherins on the tip and substrate formed an adhesive complex. When the tip was withdrawn from the substrate (at a constant velocity of 316 nm/s) a force was exerted on the bound cadherins and above a critical force the adhesive complex ruptured. Forces between the cadherin–Fc dimers were measured 7,995 times in 2.5 mM calcium, yielding 509 binding events, and 5,931 times in 2 mM EGTA, yielding 123 binding events. Forces between the cadherin monomers were measured 5,949 times in 2.5 mM calcium, yielding 113 binding events and 5,846 times in 2 mM EGTA, yielding 28 binding events.

ACKNOWLEDGMENTS. We thank Dr. Tomas Perez for help in the early stages of this project. S.S. and S.C. thank Agilent Technologies for a generous loan of an AFM 5500. This work was initially supported by the Bio-X Program at Stanford University. Work in S.C.'s laboratory is supported by grants from the National Science Foundation, the National Aeronautics and Space Administration, and the Air Force Office of Scientific Research. Work in W.J.N.'s laboratory is supported by National Institutes of Health RO1 GM35527.

1. Takeichi M (2007) The cadherin superfamily in neuronal connections and interactions. *Nat Rev Neurosci* 8:11–20.
2. Halbleib JM, Nelson WJ (2006) Cadherins in development: Cell adhesion, sorting, and tissue morphogenesis. *Genes Dev* 20:3199–3214.
3. Gumbiner BM (2005) Regulation of cadherin-mediated adhesion in morphogenesis. *Nat Rev Mol Cell Biol* 6:622–634.
4. Cowin P, Rowlands TM, Hatsell SJ (2005) Cadherins and catenins in breast cancer. *Curr Opin Cell Biol* 17:499–508.
5. Pokutta S, Weis WI (2007) Structure and mechanism of cadherins and catenins in cell–cell contacts. *Annu Rev Cell* Dev Biol 23:237–261.
6. Alberts B, *et al.* (2002) *Molecular Biology of the Cell* (Garland Science, New York).
7. Stemmler MP (2008) Cadherins in development and cancer. *Mol BioSyst* 4:835–850.
8. Niessen CM, Gottardi CJ (2008) Molecular components of the adherens junction. *Biochim Biophys Acta* 1778:562–571.
9. Niessen CM (2007) Tight junctions/adherens junctions: Basic structure and function. *J Invest Dermatol* 127:2525–2532.
10. Shapiro L, *et al.* (1995) Structural basis of cell–cell adhesion by cadherins. *Nature* 374:327–337.
11. Boggon TJ, *et al.* (2002) C-cadherin ectodomain structure and implications for cell adhesion mechanisms. *Science* 296:1308–1313.
12. Al-Amoudi A, Diez DC, Betts MJ, Frangakis AS (2007) The molecular architecture of cadherins in native epidermal desmosomes. *Nature* 450:832–838.
13. He WZ, Cowin P, Stokes DL (2003) Untangling desmosomal knots with electron tomography. *Science* 302:109–113.
14. Koch AW, Bozic D, Pertz O, Engel J (1999) Homophilic adhesion by cadherins. *Curr Opin Struct Biol* 9:275–281.
15. Pertz O, *et al.* (1999) A new crystal structure, Ca^{2+} dependence and mutational analysis reveal molecular details of E-cadherin homoassociation. *EMBO J* 18:1738–1747.
16. Sivasankar S, Gumbiner B, Leckband D (2001) Direct measurements of multiple adhesive alignments and unbinding trajectories between cadherin extracellular domains. *Biophys J* 80:1758–1768.
17. Sivasankar S, Brieher W, Lavrik N, Gumbiner B, Leckband D (1999) Direct molecular force measurements of multiple adhesive interactions between cadherin ectodomains. *Proc Natl Acad Sci USA* 96:11820–11824.
18. Zhu B, *et al.* (2003) Functional analysis of the structural basis of homophilic cadherin adhesion. *Biophys J* 84:4033–4042.
19. Chappuis-Flament S, Wong E, Hicks LD, Kay CM, Gumbiner BM (2001) Multiple cadherin extracellular repeats mediate homophilic binding and adhesion. *J Cell Biol* 154:231–243.
20. Foty RA, Steinberg MS (2005) The differential adhesion hypothesis: A direct evaluation. *Dev Biol* 278:255–263.
21. Chen CP, Posy S, Ben-Shaul A, Shapiro L, Honig BH (2005) Specificity of cell–cell adhesion by classical cadherins: Critical role for low-affinity dimerization through β-strand swapping. *Proc Natl Acad Sci USA* 102:8531–8536.
22. Tamura K, Shan WS, Hendrickson WA, Colman DR, Shapiro L (1998) Structure–function analysis of cell adhesion by neural (N-) cadherin. *Neuron* 20:1153–1163.
23. Nagar B, Overduin M, Ikura M, Rini JM (1996) Structural basis of calcium-induced E-cadherin rigidification and dimerization. *Nature* 380:360–364.
24. Tomschy A, Fauser C, Landwehr R, Engel J (1996) Homophilic adhesion of E-cadherin occurs by a cooperative 2-step interaction of N-terminal domains. *EMBO J* 15:3507–3514.
25. Brieher WM, Yap AS, Gumbiner BM (1996) Lateral dimerization is required for the homophilic binding activity of C-cadherin. *J Cell Biol* 135:487–496.
26. Haussinger D, *et al.* (2004) Proteolytic E-cadherin activation followed by solution NMR and X-ray crystallography. *EMBO J* 23:1699–1708.
27. Troyanovsky RB, Sokolov E, Troyanovsky SM (2003) Adhesive and lateral E-cadherin dimers are mediated by the same interface. *Mol Cell Biol* 23:7965–7972.
28. Troyanovsky RB, Law O, Troyanovsky SM (2007) Stable and unstable cadherin dimers: Mechanisms of formation and roles in cell adhesion. *Mol Biol Cell* 18:4343–4352.
29. Troyanovsky RB, Sokolov EP, Troyanovsky SM (2006) Endocytosis of cadherin from intracellular junctions is the driving force for cadherin adhesive dimer disassembly. *Mol Biol Cell* 17:3484–3493.
30. Perret E, Leung A, Feracci H, Evans E (2004) *Trans*-bonded pairs of E-cadherin exhibit a remarkable hierarchy of mechanical strengths. *Proc Natl Acad Sci USA* 101:16472–16477.
31. Miyaguchi K (2000) Ultrastructure of the zonula adherens revealed by rapid-freeze deep-etching. *J Struct Biol* 132:169–178.
32. Overduin M, *et al.* (1995) Solution structure of the epithelial cadherin domain responsible for selective cell adhesion. *Science* 267:386–389.
33. Nose A, Tsuji K, Takeichi M (1990) Localization of specificity determining sites in cadherin cell-adhesion molecules. *Cell* 61:147–155.
34. Vestweber D, Kemler R (1985) Identification of a putative cell-adhesion domain of uvomorulin. *EMBO J* 4:3393–3398.
35. Ozawa M, Hoschutzky H, Herrenknecht K, Kemler R (1990) A possible new adhesive site in the cell-adhesion molecule uvomorulin. *Mech Dev* 33:49–56.
36. Sandin S, Ofverstedt LG, Wikstrom AC, Wrange O, Skoglund U (2004) Structure and flexibility of individual immunoglobulin G molecules in solution. *Structure (London)* 12:409–415.
37. Saphire EO, *et al.* (2002) Contrasting IgG structures reveal extreme asymmetry and flexibility. *J Mol Biol* 319:9–18.
38. Higgins JMG, *et al.* (1998) Direct and regulated interaction of integrin α(E)β(7) with E-cadherin. *J Cell Biol* 140:197–210.
39. Baumgartner W, *et al.* (2000) Cadherin interaction probed by atomic force microscopy. *Proc Natl Acad Sci USA* 97:4005–4010.
40. Aitken CE, Marshall RA, Pulglisi JD (2008) An oxygen scavenging system for improvement of dye stability in single-molecule fluorescence experiments. *Biophys J* 94:1826–1835.
41. Rasnik I, McKinney SA, Ha T (2006) Nonblinking and long-lasting single-molecule fluorescence imaging. *Nat Methods* 3:891–893.
42. Hutter JL, Bechhoefer J (1993) Calibration of atomic-force microscope tips. *Rev Sci Instrum* 64:1868–1873.